

# $^{13}\text{C}/^{31}\text{P}$ MRS Metabolic Biomarkers of Disease Progression and Response to AAV Delivery of hGAA in a Mouse Model of Pompe Disease

Celine Baligand,<sup>1</sup> Adrian G. Todd,<sup>2</sup> Brittany Lee-McMullen,<sup>1</sup> Ravneet S. Vohra,<sup>1</sup> Barry J. Byrne,<sup>2</sup> Darin J. Falk,<sup>2,3</sup> and Glenn A. Walter<sup>1,3</sup>

<sup>1</sup>Department of Physiology and Functional Genomics, University of Florida, Gainesville, FL 32610, USA; <sup>2</sup>Department of Pediatrics, University of Florida, Gainesville, FL 32610, USA

**The development of therapeutic clinical trials for glycogen storage disorders, including Pompe disease, has called for non-invasive and objective biomarkers. Glycogen accumulation can be measured in vivo with  $^{13}\text{C}$  MRS. However, clinical implementation remains challenging due to low signal-to-noise. On the other hand, the buildup of glycolytic intermediates may be detected with  $^{31}\text{P}$  MRS. We sought to identify new biomarkers of disease progression in muscle using  $^{13}\text{C}/^{31}\text{P}$  MRS and  $^1\text{H}$  HR-MAS in a mouse model of Pompe disease (*Gaa*<sup>-/-</sup>). We evaluated the sensitivity of these MR biomarkers in vivo after treatment using an adeno-associated virus vector 2/9 encoding hGAA driven by the desmin promoter.  $^{31}\text{P}$  MRS showed significantly elevated phosphomonoesters (PMEs) in *Gaa*<sup>-/-</sup> compared to control at 2 ( $0.06 \pm 0.02$  versus  $0.03 \pm 0.01$ ;  $p = 0.003$ ), 6, 12, and 18 months of age. Correlative  $^1\text{H}$  HR-MAS measures in intact gastrocnemius muscles revealed high glucose-6-phosphate (G-6-P). After intramuscular AAV injections, glycogen, PME, and G-6-P were decreased within normal range. The changes in PME levels likely partly resulted from changes in G-6-P, one of the overlapping phosphomonoesters in the  $^{31}\text{P}$  MR spectra in vivo. Because  $^{31}\text{P}$  MRS is inherently more sensitive than  $^{13}\text{C}$  MRS, PME levels have greater potential as a clinical biomarker and should be considered as a complementary approach for future studies in Pompe patients.**

## INTRODUCTION

Glycogen storage type II, or Pompe disease, is a progressive metabolic disorder caused by a defect in the expression of acid  $\alpha$ -glucosidase (GAA), the enzyme responsible for glycogen degradation within the lysosome. The disease is characterized by glycogen accumulation in many organs including the liver, heart, diaphragm, and skeletal muscles. Dependent upon the severity of the mutation, patients are mainly affected by profound cardiac and skeletal muscle weakness and, ultimately, respiratory insufficiency and fatal heart disease.<sup>1</sup> The current standard of care consists of the management of lysosomal glycogen through enzyme replacement therapy (ERT).<sup>2</sup> Although ERT has been successful in reducing cardiac involvement and extending life expectancy, many patients still require assisted ventilation.<sup>2</sup> In addition,

bi-weekly systemic infusion of recombinant cell-derived GAA is a major burden on patients. An alternative and potentially more efficacious approach is gene therapy, which targets the underlying cause of the disease and aims to restore sustained expression of the missing gene.

Gene therapy is gaining momentum, with several ongoing clinical trials in dystrophies, including a trial recently initiated in glycogen storage disorder type II (GSDII) patients aiming at restoring GAA activity.<sup>3</sup> The current outcome measures are functional tests (6-min walking test [6MWT] and forced vital capacity [FVC])<sup>4</sup> and biochemical evaluation of biopsy samples. However, functional tests are highly dependent on subject compliance and limit the study population to ambulatory patients. Biopsies are extremely invasive and cannot capture the possible heterogeneous response to treatment throughout the muscle. Accordingly, there is an urgent need for relevant, non-invasive, and sensitive biomarkers able to probe local metabolic changes in response to treatment for Pompe disease.

In vivo nuclear magnetic resonance (NMR) has long been used in animal models and in humans for quantification of glycogen concentration and metabolism in liver and muscle in vivo.<sup>5-7</sup> In particular, NMR techniques such as  $^1\text{H}$  and  $^{13}\text{C}$  spectroscopy (MRS) have been applied in the liver and muscles of patients with various glycogen storage disorders.<sup>8-11</sup> However,  $^{13}\text{C}$  sensitivity is limited by the low natural abundance and low gyromagnetic ratio of the  $^{13}\text{C}$  nuclei compared to  $^1\text{H}$ , and the technique is still only primarily used in research settings.  $^{13}\text{C}$  detection in preclinical models, such as the genetically modified mouse models of Pompe disease (*Gaa*<sup>-/-</sup>),<sup>12,13</sup> presents even greater challenges due to the low muscle mass of the animals, and there are no reports of in vivo natural

Received 13 June 2017; accepted 5 September 2017;  
<http://dx.doi.org/10.1016/j.omtm.2017.09.002>.

<sup>3</sup>These authors contributed equally to this work.

**Correspondence:** Barry J. Byrne, Department of Pediatrics, University of Florida, P.O. Box 100296, Gainesville, FL 32610, USA.

**E-mail:** [bbyrne@ufl.edu](mailto:bbyrne@ufl.edu)

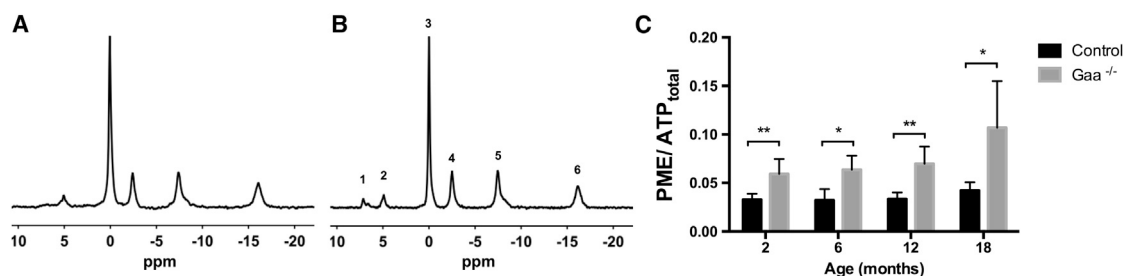


**Figure 1. In Vivo <sup>31</sup>P MRS**

Representative spectra from the lower leg muscle of (A) a control animal and (B) a *Gaa*<sup>-/-</sup> animal. The different peaks were assigned to (1) PME, (2) Pi, (3) PCr, (4) adenosine triphosphate  $\gamma$  (ATP $\gamma$ ), (5) ATP $\alpha$ , and (6) ATP $\beta$ . (C) PME levels determined by peak signal integration and expressed as PME/ATP<sub>total</sub> were significantly higher compared to age-matched controls by a factor of 2 or more in all age groups (2, 6, 12, 18 months old). Results are presented as mean  $\pm$  standard deviation. \**p* < 0.05; \*\**p* < 0.01.

abundance <sup>13</sup>C MRS glycogen in mouse skeletal muscle. Developing more sensitive <sup>13</sup>C MRS protocols and investigating alternative MR markers can potentially fulfill an unmet clinical need in glycogen storage diseases.

While GAA deficiency and subsequent increase in glycogen concentration are the primary features of the disease, recent preclinical findings demonstrated a more extensive alteration of glycogen metabolism in the *Gaa*<sup>-/-</sup> model.<sup>14</sup> Specifically, elevation of hexokinase, glycogen synthase (GS), glycogenin, and glucose-6-phosphate (G-6-P) have all been observed. This has led to the development of adjuvant substrate deprivation therapies targeting GS and glycogenin in preclinical models.<sup>15–17</sup> Therefore, the molecules involved in these metabolic processes may serve as markers of disease progression and treatment efficacy in Pompe disease. Intermediates of glucose/glycogen metabolism such as G-6-P and other high-energy phosphorylated metabolites can be quantified in vivo using <sup>31</sup>P MRS. In the past, <sup>31</sup>P MRS has been used to study glucose transport and energy metabolism in both liver<sup>18</sup> and muscle disorders.<sup>11,19–22</sup> This technique presents advantages over <sup>13</sup>C MRS, in that the <sup>31</sup>P has a higher sensitivity than <sup>13</sup>C and the NMR visible isotope is 100% naturally abundant.

Considering that the buildup of both glycogen and glycogenesis intermediates occur in Pompe skeletal muscle, we sought to implement both <sup>13</sup>C and <sup>31</sup>P MRS measurements in the *Gaa*<sup>-/-</sup> mouse model of the disease. We hypothesized that <sup>31</sup>P-MRS of phosphorylated metabolites can provide complementary biomarkers of Pompe disease progression and treatment efficacy. We implemented in vivo MRS at high field (11.1T) and non-invasively characterized the <sup>13</sup>C and <sup>31</sup>P MRS signatures of disease progression in *Gaa*<sup>-/-</sup> muscle. In addition, we evaluated the changes in MRS-detected metabolite levels in response to the expression of GAA following gene transfer using an adeno-associated virus vector 2/9 encoding hGAA driven by the desmin promoter (rAAV2/9-DES-hGAA).<sup>23</sup> The results were compared to ex vivo NMR analysis of muscle samples with <sup>1</sup>H high resolution magic angle spinning (<sup>1</sup>H HR-MAS) spectroscopy and biochemical assays on tissue homogenates to validate the in vivo measurements.

## RESULTS

### <sup>31</sup>P MRS Metabolic Signature of Disease in *Gaa*<sup>-/-</sup> Skeletal Muscle

Typical <sup>31</sup>P MR spectra obtained from the lower leg of a 6-month-old *Gaa*<sup>-/-</sup> mouse and an age-matched control are shown in Figures 1A and 1B. <sup>31</sup>P MRS data from resting muscle allowed for the determination of phosphorylated metabolite ratios and intracellular pH (pH<sub>i</sub>), thereby providing an index of the cellular energetic state. The PME signal relative to the total ATP signal (PME/ATP<sub>total</sub>) was significantly higher in *Gaa*<sup>-/-</sup> mice compared to controls at 2 months (*p* = 0.003), 6 months (*p* = 0.04), 12 months (*p* = 0.006), and 18 months of age (*p* = 0.024) (Table 1; Figure 1C). In control, PME/ATP<sub>total</sub> was not significantly different between age groups, while in *Gaa*<sup>-/-</sup> animals it was significantly different between the 2- and 18-month-old time-points (*p* = 0.008). All other metabolic indices—inorganic phosphates (Pi) to phosphocreatine (PCr) ratio (Pi/PCr) ratio, pH<sub>i</sub>, and PCr signal relative to the total ATP content (PCr/ATP<sub>total</sub>)—did not show significant differences between animal groups and across age groups (Table 1).

### rAAV2/9-DES-hGAA Induces High GAA Activity and Glycogen Clearance in *Gaa*<sup>-/-</sup> Gastrocnemius

Twenty-eight days after unilateral intramuscular injection of rAAV2/9-DES-hGAA in 2 month-old *Gaa*<sup>-/-</sup> mice (*Gaa*<sup>-/-</sup> + AAV), glycogen content was evaluated using three different types of measurements: in vivo <sup>13</sup>C MRS, ex vivo <sup>1</sup>H HR-MAS, and quantitative determination of glycogen content with biochemical assay on muscle extracts. Examples of <sup>13</sup>C MRS spectra obtained in vivo from an untreated *Gaa*<sup>-/-</sup> mouse and a naive wild-type control are shown in Figure 2.

Analysis of the glycogen peak signal-to-noise at the <sup>13</sup>C1 position (100.5 ppm) showed significantly lower glycogen levels in the treated leg compared to the untreated *Gaa*<sup>-/-</sup> (*Gaa*<sup>-/-</sup> + AAV, 3.9  $\pm$  2.1; *Gaa*<sup>-/-</sup>, 10.1  $\pm$  2.7, *p* = 0.0005; Figure 3A). This observation was consistent with <sup>1</sup>H HR-MAS NMR measurements of the glycogen peak relative to the total metabolites signal in the corresponding harvested gastrocnemius muscles (*Gaa*<sup>-/-</sup> + AAV, 0.14  $\pm$  0.07; *Gaa*<sup>-/-</sup>, 0.40  $\pm$  0.25, *p* = 0.04; Figure 3B). These results were further confirmed

**Table 1. In Vivo <sup>31</sup>P MRS Measures of Metabolites Ratios and pH<sub>i</sub> for Controls, *Gaa*<sup>-/-</sup> Untreated, and *Gaa*<sup>-/-</sup> Treated with Intramuscular Injections of rAAV2/9-DES-hGAA**

	No Treatment				rAAV Treatment
	2 Months Old	6 Months Old	12 Months Old	18 Months Old	2 Months Old
<b>pH</b>					
Control	7.13 ± 0.03	7.10 ± 0.02	7.05 ± 0.04	7.10 ± 0.03	NA
<i>Gaa</i> <sup>-/-</sup>	7.11 ± 0.02	7.05 ± 0.03	7.04 ± 0.02	7.09 ± 0.06	7.12 ± 0.06
<b>PCr/ATP<sub>total</sub></b>					
Control	0.90 ± 0.09	0.80 ± 0.04	0.68 ± 0.02	0.82 ± 0.11	NA
<i>Gaa</i> <sup>-/-</sup>	0.86 ± 0.11	0.81 ± 0.10	0.63 ± 0.04	0.7 ± 0.07	0.74 ± 0.10
<b>Pi/(Pi + PCr)</b>					
Control	0.09 ± 0.02	0.08 ± 0.02	0.10 ± 0.03	0.09 ± 0.02	NA
<i>Gaa</i> <sup>-/-</sup>	0.10 ± 0.02	0.09 ± 0.03	0.12 ± 0.01	0.13 ± 0.03	0.08 ± 0.01
<b>PME/ATP<sub>total</sub></b>					
Control	0.03 ± 0.01	0.03 ± 0.01	0.03 ± 0.01	0.04 ± 0.01	NA
<i>Gaa</i> <sup>-/-</sup>	0.06 ± 0.02**	0.06 ± 0.01*	0.07 ± 0.02**	0.11 ± 0.05*	0.04 ± 0.01 <sup>#</sup>

No difference in PCr/ATP<sub>total</sub>, Pi/(Pi + PCr), or pH<sub>i</sub> were found between groups. PME/ATP<sub>total</sub> was significantly higher in *Gaa*<sup>-/-</sup> compared to control for all age groups (2, 6, 12, 18 months old). PME/ATP<sub>total</sub> were significantly lower in *Gaa*<sup>-/-</sup> after treatment compared to untreated legs. \*p < 0.05 compared to age-matched control; \*\*p < 0.006 compared to age-matched control; <sup>#</sup>p = 0.03 compared to untreated leg.

by biochemical assessment, where glycogen concentration in the treated leg was significantly lower as compared to the untreated leg (*Gaa*<sup>-/-</sup> + AAV, 20.2 ± 9.1; *Gaa*<sup>-/-</sup>, 56.4 ± 14.1 μg/mL; p = 0.0001; Figure 3C) but was not significantly different from control values (control, 9.5 ± 5.0 μg/mL).

rAAV2/9-DES-hGAA injections resulted in higher GAA enzymatic activity compared to the untreated leg, with values ranging from 3 to 107 nmol/hr/mg (Figure 4A). Activity levels were significantly lower in *Gaa*<sup>-/-</sup> (p < 0.0001) as compared to control values and significantly higher in *Gaa*<sup>-/-</sup> + AAV as compared to *Gaa*<sup>-/-</sup> (p = 0.03).

Taking advantage of the range of GAA activity achieved post-gene-transfer, we looked at the relationship between the glycogen measures normalized to the maximum measured value and enzymatic activity for each technique. We observed that glycogen levels were highly correlated to GAA activity and rapidly decreased with increasing GAA activity (biochemical assay—Spearman r = -0.96, p < 0.0001; <sup>1</sup>H HR-MAS—r = -0.85, p = 0.0006; <sup>13</sup>C MRS—r = -0.71, p = 0.013; Figures 4B and 5). Glycogen content determined by biochemical assay could be fitted to an exponential decay as a function of GAA activity as shown on Figure 5. Enzymatic activity above 10 nmol/hr/mg did not induce a larger decrease and all three types of measures plateaued at wild-type control values.

#### **PME/ATP<sub>total</sub> and G-6-P Signal Decrease in Response to rAAV2/9-DES-hGAA**

<sup>31</sup>P MRS measurements showed that PME/ATP<sub>total</sub> was significantly lower in *Gaa*<sup>-/-</sup> + AAV than in naive *Gaa*<sup>-/-</sup> mice (*Gaa*<sup>-/-</sup> + AAV, 0.037 ± 0.006; *Gaa*<sup>-/-</sup>, 0.059 ± 0.015, p = 0.03). In addition, *Gaa*<sup>-/-</sup> +

AAV values were not statistically different from control (0.032 ± 0.006; ns) (Figure 6). G-6-P signal detected by <sup>1</sup>H HR-MAS relative to the total signal was significantly higher in *Gaa*<sup>-/-</sup> when compared to controls (0.58 ± 0.12 versus 0.35 ± 0.09; p = 0.03). Similar to PME, G-6-P levels were lower in *Gaa*<sup>-/-</sup> + AAV compared to *Gaa*<sup>-/-</sup> (0.41 ± 0.03; p = 0.03) and not different from controls (p = 0.33).

#### **DISCUSSION**

For the first time, we have demonstrated the significance of MRS to detect highly concentrated phosphorylated metabolites for the non-invasive evaluation of disease progression and treatment efficacy in the muscles of a validated preclinical model of Pompe disease. First, we observed that the phosphomonoester (PME) <sup>31</sup>P MRS signal was elevated in the skeletal muscle of *Gaa*<sup>-/-</sup> mice and throughout the lifespan of the animal. Second, we showed that restoration of normal to high levels of GAA activity using an AAV-based approach resulted in a decrease in <sup>31</sup>P MRS PME signal. These changes were concomitant to the glycogen clearance expected with increased GAA activity, as measured by <sup>13</sup>C MRS in vivo, <sup>1</sup>H HRMAS of muscle samples, and by the biochemical determination of glycogen content in muscle extracts. In addition, we showed that the changes in PME signal detected in vivo could be potentially explained by changes in glucose-6-phosphate, one of the contributors to the <sup>31</sup>P PME signal.

A major finding of this study is that elevated <sup>31</sup>P MRS PME signal can be detected in vivo in *Gaa*<sup>-/-</sup> mice skeletal muscle. As early as 2 months of age, PME levels were 60% higher in *Gaa*<sup>-/-</sup> as compared to control muscles, and remained elevated throughout the 18 months of our study. Multiple overlapping resonances contribute to the MR signal in the PME region, including phosphocholine, phosphoethanolamine and glycolytic intermediates (glucose-6-P, fructose-6-P),

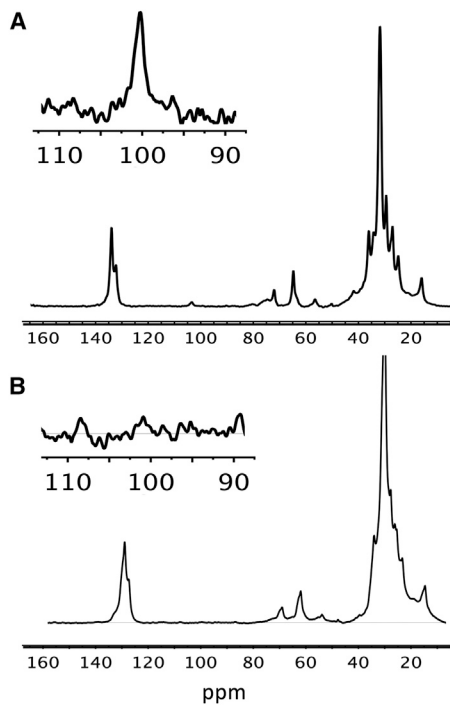


**Figure 2. In Vivo  $^{13}\text{C}$  MRS**

Representative in vivo  $^{13}\text{C}$  MR spectra acquired from the lower leg muscles of a  $Gaa^{-/-}$  mouse (A) and a control mouse (B) in vivo. The inserts show a zoom on the 90 to 110 ppm region, with the C1 glycogen resonance at 100.5 ppm. No signal could be detected in control animals due to very low glycogen concentrations. The other peaks are largely dominated by signal from the lipids overlapping with other resonances such as other glycogen carbons, creatine, taurine, and other sugars.

that could not be resolved by  $^{31}\text{P}$  MRS in vivo. Therefore, we performed ex vivo analysis using  $^1\text{H}$  high resolution magic angle spectroscopy ( $^1\text{H}$  HR-MAS), which allows for the acquisition of high resolution NMR spectra in intact tissues and can be used specifically for the determination of phosphate sugars.<sup>24</sup> With this technique, we found a significantly higher G-6-P signal in the spectra, suggesting a large contribution of G-6-P to the change in PME signal in vivo. G-6-P is at a key intersection of glucose utilization pathways, namely glycolysis, pentose-phosphate, and glycogenesis pathways. It is also a direct product of glycogenolysis. Accordingly, high G-6-P levels are compatible with the high cytoplasmic glycogen concentration in Pompe disease.<sup>25,26</sup> Since G-6-P is known as an activator of GS,<sup>27</sup> it is possible that the increase in GAA activity with rAAV2/9-DES-hGAA treatment initiated a cycle in which glycogen clearance results in lower G-6-P levels and, in turn, in lower glycogen production through GS. These multiple roles of G-6-P make PME levels an attractive marker of the metabolic changes associated with Pompe disease progression and treatment that can be detected non-invasively by in vivo  $^{31}\text{P}$  MRS.

The primary hallmark of Pompe disease progression is the increase in lysosomal and cytosolic glycogen concentration. Because the C1 glycogen peak detected by  $^{13}\text{C}$  MRS can be unequivocally identified

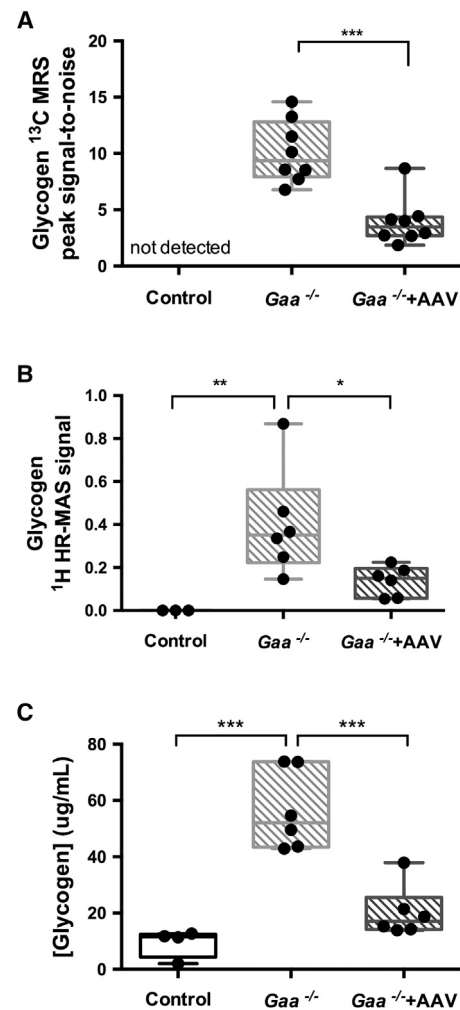


**Figure 3. Glycogen Measurements**

Measures of glycogen levels (A) with  $^{13}\text{C}$  MRS in vivo, (B) with  $^1\text{H}$  HR-MAS of intact muscles, and (C) with quantitative biochemical assays of muscle extracts in  $\mu\text{g}/\text{mL}$ . All three types of measurements showed significantly higher glycogen levels in  $Gaa^{-/-}$  compared to controls and significantly lower glycogen level after rAAV2/9-DES-hGAA treatment ( $Gaa^{-/-}$  + AAV) as compared to untreated  $Gaa^{-/-}$ . Data are presented as individual data points and box plots indicating the lower and upper quartiles and the median. The bars indicate the minimum and maximum values. \* $p < 0.05$ ; \*\* $p < 0.01$ ; \*\*\* $p < 0.001$ .

at 100.5 ppm, and with the availability of higher field strength clinical scanner,<sup>28</sup> natural abundance  $^{13}\text{C}$  MRS has become a method of choice for clinical research studies of glycogen storage disorders. However, it remains challenging to perform such measurements in transgenic mouse models because of the small size of the animal, especially in skeletal muscles where glycogen content is much lower than in the liver. Here, we were able to detect glycogen in the lower leg of  $Gaa^{-/-}$  mice using in vivo MRS and a simple surface coil set-up at 11.1T. However, unlike PME levels, glycogen could not be reliably measured in control mice due to low signal-to-noise ratio. Even at 11.1T, long acquisition times were necessary even in  $Gaa^{-/-}$  mice

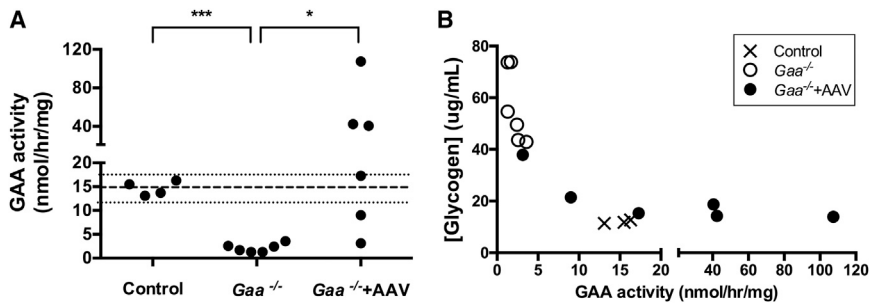


**Figure 4. Effect of rAAV2/9-DES-hGAA Treatment on GAA Activity and Glycogen Concentration**

Glycogen concentration in  $\mu\text{g/mL}$  determined by biochemical assay on muscle homogenates for control, *Gaa*<sup>-/-</sup>, and *Gaa*<sup>-/-</sup> + AAV (A) and as a function of GAA activity (B). The dashed lines represent the average control value and the upper and lower 95% confidence interval. GAA activity of 10 nmol/hr/mg was sufficient to induce glycogen clearance. GAA activity above that value did not induce lower glycogen concentrations than found in control animals. \* $p = 0.03$ , \*\*\* $p < 0.0001$ .

with high glycogen concentration (1 hr). To address this limitation, future <sup>13</sup>C MRS preclinical studies may benefit from the use of a higher magnetic field strength, the development of more sensitive RF coils,<sup>29</sup> dynamic polarization, and possibly the use of <sup>13</sup>C enriched substrates. Nonetheless, we were able to detect changes in glycogen level in vivo after AAV treatment, and all glycogen measures showed a significant and consistent response to treatment 28 days after AAV injection, with an average decrease of 61%, 66% and 64% for MRS, HR-MAS, and biochemical assays, respectively.

We previously reported that intra-muscular injection of rAAV2/9-DES-hGAA could restore GAA expression in the TA muscle.<sup>23</sup> Here, we successfully modified this protocol to treat a larger part of the leg, including the TA and both heads of the gastrocnemius. We found that GAA activity was restored to control values at or above endogenous levels in the gastrocnemius, where muscle wet weight is typically more than twice that of the TA. Significant glycogen clearance was achieved within 28 days post AAV delivery. This strategy was also motivated by the fact that the MRS acquisitions performed in this study were not spatially selective. The entire leg contributed to the observed signal <sup>31</sup>P and <sup>13</sup>C signal, with a larger contribution of the posterior compartment (i.e. gastrocnemius and soleus). This limitation is specific to small animal studies and can easily be overcome in human studies, where <sup>31</sup>P chemical shift imaging has been implemented, including in muscular dystrophies.<sup>22,30,31</sup>

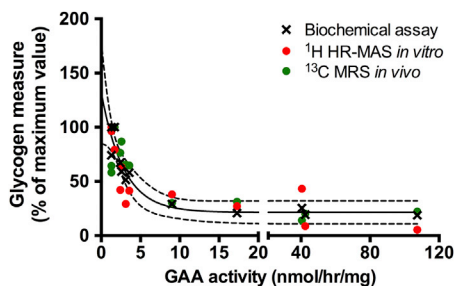


**Figure 5. Relationship between Glycogen Levels and GAA Activity**

Overlay of the results obtained from the three different glycogen measurements as a function of the corresponding GAA concentration. The solid black line represents the result of a fit of the quantitative measurements by biochemical assay to a monoexponential decay, and the dashed lines represent the 95% confidence interval of the fit. Values are normalized to their maximum for display purposes.

From a technical standpoint, the increasing availability of high field multinuclei hardware in research centers combined with the much higher SNR achievable in human compared to mice makes the clinical translation of these MR measures readily feasible. Indeed, the <sup>31</sup>P MRS measurement of muscle phosphodiesterases (PDE) has been shown to be a biomarker for Duchenne and Becker muscular dystrophy.<sup>22,32</sup> A recent study by Le Guiner et al. in dystrophic dogs showed that Pi/ATP and PDE levels were sensitive to intramuscular delivery of rAAV2/8 encoding a canine microdystrophin.<sup>33</sup> However, a limitation of our approach is that <sup>13</sup>C and <sup>31</sup>P markers are modulated by both AAV transduction success and heterogeneity of treatment distribution within a given volume of tissue. This is inherent to any volume-averaged measure and cannot be easily overcome. In addition, the ideal surrogate biomarker for Pompe disease should have a high and preferably close to linear sensitivity to moderate changes in either or both glycogen concentration and GAA activity. Further investigation is therefore warranted to determine the exact level of sensitivity of the proposed <sup>13</sup>C and <sup>31</sup>P markers within the specific range of values observed in humans.

In conclusion, our findings show that metabolic changes involving phosphorylated metabolites in parallel to glycogen accumulation can be probed in vivo in *Gaa*<sup>-/-</sup> mice using <sup>31</sup>P MRS. Specifically, elevated PME levels are a characteristic of the disease and sensitive to the response to rAAV2/9-DES-hGAA intramuscular injections. Because the sensitivity of <sup>31</sup>P MRS is superior to that of <sup>13</sup>C MRS, PME levels have great potential as a clinical biomarker and should be considered as a complementary approach for future studies in Pompe patients.

## MATERIALS AND METHODS

### Animals

All procedures were performed in accordance with the U.S. Government Principle for the Utilization and Care of Vertebrate Animals and were approved by the University of Florida's Institutional Animal Care & Use Committee.

Male and female *Gaa*<sup>-/-</sup> mice (Taconic, Germantown, NY) originally developed by Raben et al.<sup>13</sup> were outbred to a 129SVE background. *Gaa*<sup>-/-</sup> mice and age-matched control wild-type 129SVE mice, (Taconic, Germantown, NY) were studied at 2 months (*Gaa*<sup>-/-</sup>,  $n = 6$ ; control,  $n = 6$ ), 6 months (*Gaa*<sup>-/-</sup>,  $n = 3$ ; control,  $n = 3$ ), 12 months

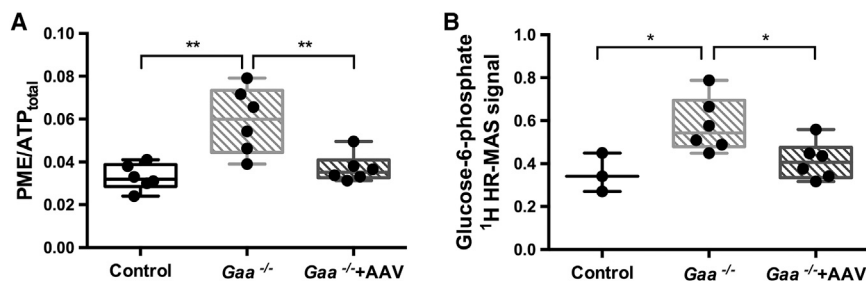


**Figure 6. Effect of rAAV2/9-DES-hGAA Treatment on <sup>31</sup>P MRS PME Resonances In Vivo and <sup>1</sup>H HR-MAS Glucose-6-Phosphate in Isolated Muscles**

Both in vivo PME levels and glucose-6-phosphate levels from intact muscles were significantly elevated in *Gaa*<sup>-/-</sup> mice compared to control. rAAV2/9-DES-hGAA induced a significant decrease in both PME (A) and glucose-6-phosphate (B). Data are presented as individual data points and box plots indicating the lower and upper quartiles and the median. The bars indicate the minimum and maximum values. \**p* < 0.05; \*\**p* < 0.005.

(*Gaa*<sup>-/-</sup>, *n* = 5; control, *n* = 4), and 18 months of age (*Gaa*<sup>-/-</sup>, *n* = 8; control, *n* = 4). A separate group of 6 *Gaa*<sup>-/-</sup> animals received unilateral intramuscular injections of rAAV2/9-DES-hGAA at three different locations in the lower leg (*Gaa*<sup>-/-</sup> + AAV). The gastrocnemius medial, the gastrocnemius lateral head, and the tibialis anterior each received a dose of  $5 \times 10^{14}$  vg/kg of tissue diluted in 50  $\mu$ L, 50  $\mu$ , and 25  $\mu$ L, respectively (Figure 7). The tibialis anterior and gastrocnemius were assumed to be representative of 0.1% and 0.3% of the animal body weight, respectively.

### <sup>31</sup>P/<sup>13</sup>C MR Spectroscopy Acquisitions In Vivo

Acquisitions were performed in an 11.1T/470MHz Agilent system (Agilent, Inc., Palo Alto, CA) using the VnmrJ 2.3 software. Animals were placed prone on a water-heated cradle, and anesthesia was ensured through a nose cone delivering an isoflurane-oxygen mixture (2%, 1 L/min).

For phosphorus spectroscopy, a single turn  $10 \times 8$  mm oval <sup>31</sup>P surface coil was placed over the belly of the lower leg posterior compartment. A 12 mm diameter <sup>1</sup>H surface coil was placed on the side of the leg, perpendicular to the <sup>31</sup>P coil, and used for positioning and shimming. After manual voxel shimming, spectra were accumulated for 5 min at the Ernst angle calibrated on PCr with a 20  $\mu$ s broad pulse and a repetition time (TR) of 1 s. Acquisition bandwidth was 10 kHz with a 2,048 point free induction decay. The carrier frequency was set to -4.5 ppm with reference to the PCr peak. A fully relaxed spectrum was acquired (TR = 15 s) to determine T1 saturation effect for each of the metabolites.

For carbon spectroscopy, a similar set up was used with a single turn  $10 \times 8$  mm oval <sup>13</sup>C surface coil. Spectra were acquired with a single 7.2  $\mu$ s broad pulse calibrated at the Ernst angle for TR = 1 s and a WALTZ-16 <sup>1</sup>H decoupling scheme<sup>34</sup> and accumulated for 1 hr. For each spectrum, a 1,024 point free induction decay (FID) was acquired over 33 ms leading to an acquisition bandwidth of 30 kHz.

### <sup>31</sup>P/<sup>13</sup>C MR Spectroscopy Data Analysis

All spectra were processed using MestReNova version 11.0.4 (Mestrelab Research S.L., Norwich, CT). After zero filling to 4,096 points, 25 Hz exponential apodization, zero and first order phasing and baseline correction, PCr frequency was set to 0 ppm on the <sup>31</sup>P spectra and peak integration of over the following chemical shifts was used to determine the relative concentrations of PME (7.8 to 5.8 ppm), Pi (5.6 to 3.6 ppm), PCr (1 to -1 ppm),  $\gamma$ - (1.5 to -3.8 ppm),  $\alpha$ - (-6.5 to -9 ppm), and  $\beta$ -ATP (-14.8 to -17.8 ppm). In addition, pHi was determined using the relative chemical shift difference between Pi and PCr resonances according to the following formula  $pH = 6.75 + \log((3.27 - \delta Pi)/(\delta Pi - 5.69))$ .<sup>35</sup> To account for partial saturation, the amplitude of each component was multiplied by the appropriate correction factor derived from fully relaxed spectra, and results are reported as the relative concentrations of Pi, PCr,  $\gamma$ -,  $\alpha$ -, and  $\beta$ -ATP. <sup>13</sup>C spectra were processed similarly. After zero filling to 2,048 points, 50 Hz exponential apodization, zero and first-order phasing and baseline correction, the glycogen peak was integrated over 2 ppm around 100.5 ppm, and results are reported as C1-glycogen peak-to-noise ratio.

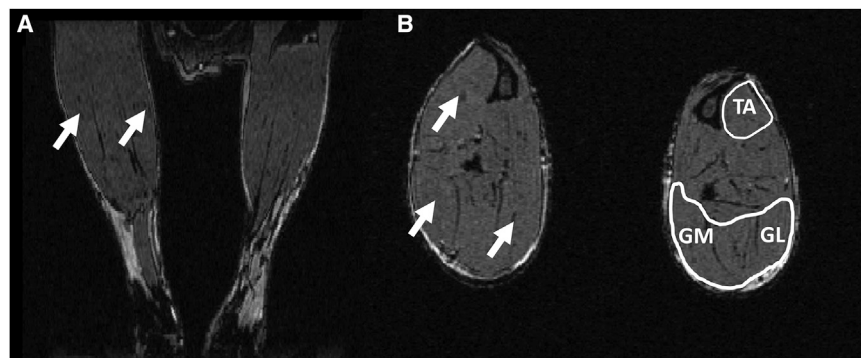


**Figure 7. Description of the rAAV2/9-DES-hGAA Injection Sites**

Representative coronal (A) and axial (B) images from a 3D T1 weighted MR image of the lower legs of a *Gaa*<sup>-/-</sup> animal are shown. The fascia appear in black on the images. The muscles are delineated in white, and the white arrows indicate the three rAAV2/9-DES-hGAA injection sites (TA, tibialis anterior; GM, medial gastrocnemius; GL, lateral gastrocnemius). 3D T1 weighted images were obtained using a gradient echo sequence on with 4.7T Agilent scanner (Agilent, Inc., Palo Alto, CA) and a custom build 3 cm-diameter <sup>1</sup>H volume coil. TR/TE = 50/7 ms, field of view =  $1.5 \times 1.8 \times 1.8$  cm<sup>3</sup>, matrix size =  $256 \times 192 \times 96$ .

### <sup>1</sup>H HR-MAS Spectroscopy

Gastrocnemius tissue from 2-month-old control ( $n = 3$ ),  $Gaa^{-/-}$  ( $n = 3$ ), and  $Gaa^{-/-}$  + AAV mice ( $n = 6$ , both legs) were analyzed using high-resolution magic-angle spinning (<sup>1</sup>H HR-MAS) NMR. Material preparation and data acquisition followed the protocols from Beckonert et al.<sup>36</sup> A portion of the tissue sample ( $25 \pm 2$  mg) was soaked in D<sub>2</sub>O and transferred into a 40  $\mu$ L rotor. <sup>1</sup>H HR-MAS data were acquired using a 4 mm probe on a 600 MHz Bruker spectrometer (Bruker, Billerica, MA) with Topspin 3.2 software. The magic angle, 54.7°, was calibrated using potassium bromide once at the beginning of the run. Pulse calibration, tune, match, and manual shimming were performed for each sample. The data was acquired using noesypr1d pulse sequence with 128 scans accumulation, spectral width of 10 ppm, 16k data points, a relaxation delay of 2 s, and mixing time of 90 ms. Spectra were processed in MestreNova 10.0 using an exponential window function with a 0.5 Hz line broadening and zero-filled to 16k. All spectra were then phased individually. Processed HR-MAS spectra were globally aligned to creatine at 3.02 ppm, and the glycogen and G-6-P resonances were identified at 5.4 and 5.22 ppm, respectively, as previously published<sup>24</sup> and as was confirmed by “spiking” a sample using a glycogen solution and a G-6-P solution. Metabolites were quantified using the MestreNova 10.0 Simple Mixture Analysis (SMA) plugin and normalized to the total signal.

### Biochemical Assays

Quantitative measurement of glycogen content was performed on gastrocnemius samples using the Glycogen Assay Kit (ab65620; Abcam, Cambridge, MA) and following the manufacturer’s instructions. GAA activity was assessed in gastrocnemius tissue lysates. The amount of 4-methylumbelliferyl- $\alpha$ -D-glucoside released by cleavage after 1 hr incubation at 37°C was measured using a commercially available kit (Sigma M9766; Sigma), as previously described.<sup>37</sup>

### Statistical Analysis

All analyses were performed using GraphPad Prism version 6.00 for Mac OS X (GraphPad Software, La Jolla, CA). To describe the differences between  $Gaa^{-/-}$  and age-matched controls, unpaired two-tailed t tests with Holm-Sidak correction for multiple comparisons were used. When comparing controls,  $Gaa^{-/-}$ -treated and  $Gaa^{-/-}$ -untreated groups, a one-way ANOVA with Holm-Sidak correction for multiple comparisons was used. To compare the results obtained from  $Gaa^{-/-}$ -treated and -untreated legs only, a Wilcoxon matched-pairs signed-rank test was used. Correlations between measures were assessed with a Pearson r test. Significance level was set to 0.05. All results are reported as mean  $\pm$  standard deviation.

### AUTHOR CONTRIBUTIONS

C.B. was responsible for the conception and design of the experiments, performed the experiments, analyzed the data, interpreted the results, and prepared the figures and manuscript. AG.T., B.L.-M., and R.S.V. performed the experiments and analyzed the data. D.J.F., B.J.B., and G.A.W. were responsible for the conception and design of the experiments, interpreted the results, and reviewed and approved the manuscript.

### ACKNOWLEDGMENTS

This work was funded by the Muscular Dystrophy Association (#MDA218585) development research grant to C.B., the National High Magnetic Field Laboratory (NHMFLP021453), the P01 HL59412 to B.J.B. and G.A.W., the Southeast Center for Integrative Metabolomics (U24 DK097209), and NIAMS (K01AR066077) to D.J.F. A portion of this work was performed in the McKnight Brain Institute at the National High Magnetic Field Laboratory’s AMRIS Facility, which is supported by National Science Foundation Cooperative Agreement No. DMR-1157490 and the State of Florida. The authors would like to thank Denise Cloutier, James Rocca, and Dr. Huadong Zeng for their technical assistance.

### REFERENCES

- Hirschhorn, R., and Reuser, A.J.J. (2001). Glycogen storage disease type II: acid alpha-glucosidase (acid maltase) deficiency. In *The Metabolic and Molecular Bases of Inherited Disease*, Vol. 3, C.R. Scriver, W.S. Sly, B. Childs, A.L. Beaudet, D. Valle, K.W. Kinzler, and B. Vogelstein, eds. (McGraw-Hill), pp. 3389–3420.
- Byrne, B.J., Kishnani, P.S., Case, L.E., Merlini, L., Müller-Felber, W., Prasad, S., and van der Ploeg, A. (2011). Pompe disease: design, methodology, and early findings from the Pompe Registry. *Mol. Genet. Metab.* 103, 1–11.
- Smith, B.K., Collins, S.W., Conlon, T.J., Mah, C.S., Lawson, L.A., Martin, A.D., Fuller, D.D., Cleaver, B.D., Clément, N., Phillips, D., et al. (2013). Phase I/II trial of adeno-associated virus-mediated alpha-glucosidase gene therapy to the diaphragm for chronic respiratory failure in Pompe disease: initial safety and ventilatory outcomes. *Hum. Gene Ther.* 24, 630–640.
- Lachmann, R., and Schoser, B. (2013). The clinical relevance of outcomes used in late-onset Pompe disease: can we do better? *Orphanet J. Rare Dis.* 8, 160.
- Shulman, R.G., and Rothman, D.L. (2001). <sup>13</sup>C NMR of intermediary metabolism: implications for systemic physiology. *Annu. Rev. Physiol.* 63, 15–48.
- Garlick, P.B., and Pritchard, R.D. (1993). Absolute quantification and NMR visibility of glycogen in the isolated, perfused rat heart using <sup>13</sup>C NMR spectroscopy. *NMR Biomed.* 6, 84–88.
- Jue, T., Rothman, D.L., Tavittian, B.A., and Shulman, R.G. (1989). Natural-abundance <sup>13</sup>C NMR study of glycogen depletion in human liver and muscle. *Proc. Natl. Acad. Sci. USA* 86, 1439–1442.
- Beckmann, N., Seelig, J., and Wick, H. (1990). Analysis of glycogen storage disease by in vivo <sup>13</sup>C NMR: comparison of normal volunteers with a patient. *Magn. Reson. Med.* 16, 150–160.
- Roser, W., Beckmann, N., Wiesmann, U., and Seelig, J. (1996). Absolute quantification of the hepatic glycogen content in a patient with glycogen storage disease by <sup>13</sup>C magnetic resonance spectroscopy. *Magn. Reson. Imaging* 14, 1217–1220.
- Wary, C., Laforêt, P., Eymard, B., Fardeau, M., Leroy-Willig, A., Bassez, G., Leroy, J.P., Caillaud, C., Poenaru, L., and Carlier, P.G. (2003). Evaluation of muscle glycogen content by <sup>13</sup>C NMR spectroscopy in adult-onset acid maltase deficiency. *Neuromuscul. Disord.* 13, 545–553.
- Wary, C., Nadaj-Pakleza, A., Laforêt, P., Claeys, K.G., Carlier, R., Monnet, A., Fleury, S., Baligand, C., Eymard, B., Labrune, P., and Carlier, P.G. (2010). Investigating glycogenosis type III patients with multi-parametric functional NMR imaging and spectroscopy. *Neuromuscul. Disord.* 20, 548–558.
- Bijvoet, A.G., van de Kamp, E.H., Kroos, M.A., Ding, J.H., Yang, B.Z., Visser, P., Bakker, C.E., Verbeet, M.P., Oostra, B.A., Reuser, A.J., and van der Ploeg, A.T. (1998). Generalized glycogen storage and cardiomegaly in a knockout mouse model of Pompe disease. *Hum. Mol. Genet.* 7, 53–62.
- Raben, N., Nagaraju, K., Lee, E., Kessler, P., Byrne, B., Lee, L., LaMarca, M., King, C., Ward, J., Sauer, B., and Plotz, P. (1998). Targeted disruption of the acid alpha-glucosidase gene in mice causes an illness with critical features of both infantile and adult human glycogen storage disease type II. *J. Biol. Chem.* 273, 19086–19092.

14. Taylor, K.M., Meyers, E., Phipps, M., Kishnani, P.S., Cheng, S.H., Scheule, R.K., and Moreland, R.J. (2013). Dysregulation of multiple facets of glycogen metabolism in a murine model of Pompe disease. *PLoS ONE* 8, e56181.
15. Douillard-Guilloux, G., Raben, N., Takikita, S., Batista, L., Caillaud, C., and Richard, E. (2008). Modulation of glycogen synthesis by RNA interference: towards a new therapeutic approach for glycogenosis type II. *Hum. Mol. Genet.* 17, 3876–3886.
16. Douillard-Guilloux, G., Raben, N., Takikita, S., Ferry, A., Vignaud, A., Guillet-Deniau, I., Favier, M., Thurberg, B.L., Roach, P.J., Caillaud, C., and Richard, E. (2010). Restoration of muscle functionality by genetic suppression of glycogen synthesis in a murine model of Pompe disease. *Hum. Mol. Genet.* 19, 684–696.
17. Clayton, N.P., Nelson, C.A., Weeden, T., Taylor, K.M., Moreland, R.J., Scheule, R.K., Phillips, L., Leger, A.J., Cheng, S.H., and Wentworth, B.M. (2014). Antisense oligonucleotide-mediated suppression of muscle glycogen synthase 1 synthesis as an approach for substrate reduction therapy of Pompe disease. *Mol. Ther. Nucleic Acids* 3, e206.
18. Oberhaensli, R., Rajagopalan, B., Galloway, G.J., Taylor, D.J., and Radda, G.K. (1990). Study of human liver disease with P-31 magnetic resonance spectroscopy. *Gut* 31, 463–467.
19. Siciliano, G., Rossi, B., Martini, A., Angelini, C., Martinuzzi, A., Lodi, R., Zaniol, P., Barbiroli, B., and Muratorio, A. (1995). Myophosphorylase deficiency affects muscle mitochondrial respiration as shown by 31P-MR spectroscopy in a case with associated multifocal encephalopathy. *J. Neurol. Sci.* 128, 84–91.
20. Barnes, P.R., Kemp, G.J., Taylor, D.J., and Radda, G.K. (1997). Skeletal muscle metabolism in myotonic dystrophy A 31P magnetic resonance spectroscopy study. *Brain* 120, 1699–1711.
21. de Haan, J.H., Klomp, D.W., Tack, C.J., and Heerschap, A. (2003). Optimized detection of changes in glucose-6-phosphate levels in human skeletal muscle by 31P MR spectroscopy. *Magn. Reson. Med.* 50, 1302–1306.
22. Hooijmans, M.T., Niks, E.H., Burakiewicz, J., Verschuuren, J.J., Webb, A.G., and Kan, H.E. (2017). Elevated phosphodiester and T2 levels can be measured in the absence of fat infiltration in Duchenne muscular dystrophy patients. *NMR Biomed.* 30, 30.
23. Todd, A.G., McElroy, J.A., Grange, R.W., Fuller, D.D., Walter, G.A., Byrne, B.J., and Falk, D.J. (2015). Correcting neuromuscular deficits with gene therapy in Pompe disease. *Ann. Neurol.* 78, 222–234.
24. Diserens, G., Vermathen, M., Gjuroski, I., Eggmann, S., Precht, C., Boesch, C., and Vermathen, P. (2016). Direct determination of phosphate sugars in biological material by <sup>1</sup>H high-resolution magic-angle-spinning NMR spectroscopy. *Anal. Bioanal. Chem.* 408, 5651–5656.
25. Garancis, J.C. (1968). Type II glycogenosis. Biochemical and electron microscopic study. *Am. J. Med.* 44, 289–300.
26. Thurberg, B.L., Lynch Maloney, C., Vaccaro, C., Afonso, K., Tsai, A.C., Bossen, E., Kishnani, P.S., and O'Callaghan, M. (2006). Characterization of pre- and post-treatment pathology after enzyme replacement therapy for Pompe disease. *Lab. Invest.* 86, 1208–1220.
27. Adeva-Andany, M.M., González-Lucán, M., Donapetry-García, C., Fernández-Fernández, C., and Ameneiros-Rodríguez, E. (2016). Glycogen metabolism in humans. *BBA Clin.* 5, 85–100.
28. Heinicke, K., Dimitrov, I.E., Romain, N., Cheshkov, S., Ren, J., Malloy, C.R., and Haller, R.G. (2014). Reproducibility and absolute quantification of muscle glycogen in patients with glycogen storage disease by <sup>13</sup>C NMR spectroscopy at 7 Tesla. *PLoS ONE* 9, e108706.
29. Kovacs, H., Moskau, D., and Spraul, M. (2005). Cryogenically cooled probes—a leap in NMR technology. *Prog. Nucl. Magn. Reson. Spectrosc.* 46, 131–155.
30. Valković, L., Chmelík, M., Meyerspeer, M., Gagoski, B., Rodgers, C.T., Krššák, M., Andronesi, O.C., Trattig, S., and Bogner, W. (2016). Dynamic (31) P-MRSI using spiral spectroscopic imaging can map mitochondrial capacity in muscles of the human calf during plantar flexion exercise at 7 T. *NMR Biomed.* 29, 1825–1834.
31. Wilhelm, T., and Bachert, P. (2001). In vivo 31P echo-planar spectroscopic imaging of human calf muscle. *J. Magn. Reson.* 149, 126–130.
32. Wokke, B.H., Hooijmans, M.T., van den Bergen, J.C., Webb, A.G., Verschuuren, J.J., and Kan, H.E. (2014). Muscle MRS detects elevated PDE/ATP ratios prior to fatty infiltration in Becker muscular dystrophy. *NMR Biomed.* 27, 1371–1377.
33. Le Guiner, C., Servais, L., Montus, M., Larcher, T., Fraysse, B., Moullec, S., Allais, M., François, V., Dutilleul, M., Malerba, A., et al. (2017). Long-term microdystrophin gene therapy is effective in a canine model of Duchenne muscular dystrophy. *Nat. Commun.* 8, 16105.
34. Shaka, A.J., Keeler, J., Frenkiel, T., and Freeman, R. (1983). An improved sequence for broadband decoupling: WALTZ-16. *J. Magn. Reson.* 52, 335–338.
35. Taylor, D.J., Bore, P.J., Styles, P., Gadian, D.G., and Radda, G.K. (1983). Bioenergetics of intact human muscle. A 31P nuclear magnetic resonance study. *Mol. Biol. Med.* 1, 77–94.
36. Beckonert, O., Coen, M., Keun, H.C., Wang, Y., Ebbels, T.M., Holmes, E., Lindon, J.C., and Nicholson, J.K. (2010). High-resolution magic-angle-spinning NMR spectroscopy for metabolic profiling of intact tissues. *Nat. Protoc.* 5, 1019–1032.
37. Falk, D.J., Mah, C.S., Soustek, M.S., Lee, K.Z., Elmallah, M.K., Cloutier, D.A., Fuller, D.D., and Byrne, B.J. (2013). Intrapleural administration of AAV9 improves neural and cardiorespiratory function in Pompe disease. *Mol. Ther.* 21, 1661–1667.